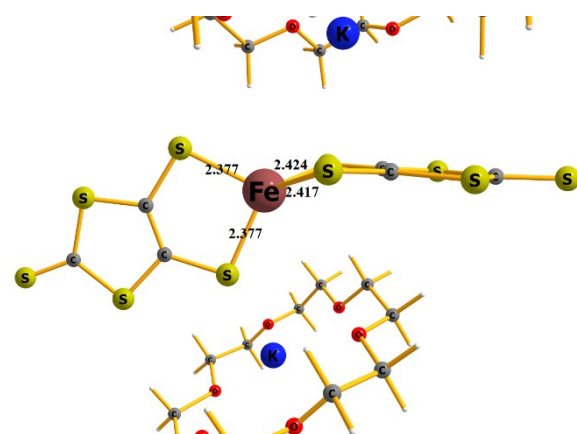


SUPPORTING INFORMATION

Computational Details:

Ab initio calculations: All the first principle calculations have been performed in ORCA 3.0.3 programme package. To get the starting orbitals, DFT (Density Functional Theory) has been performed with ROKS/BP86 method with def2-TZVP basis set on Fe, S and def2-TZVP(-f) basis set for C. In the configuration interaction (CI) step, state averaged complete active space self-consistent field (SA-CASSCF) have been carried out with 5 quintets and 45 triplets considering 6 active metal electrons in 5 metal d-orbitals. Along with this, calculations were also computed with considering 22 singlets to see whether this effects to the energy levels or not. To account for the dynamic correlation N-electron valence perturbation theory (NEVPT2) was performed on the top of CASSCF wavefunction. Relativistic effects were taken into account with considering zeroth-order regular approximation (ZORA) method which was used both in the Hamiltonian as well as in basis functions. Spin orbit interactions were accounted with quasi-degenerate perturbation theory (QDPT) as implemented in ORCA. No geometry optimization was performed as we found that gas phase as well as solvent phase optimization leads to significant distortion of the molecular geometry.



For example, optimization of complex 1 leads to loss of planarity as well as lose of bond angles and dihedral angles from the original X-Ray structures. It shows D and E/D values of $\pm 5 \text{ cm}^{-1}$ and 0.32 respectively.

DFT calculations: To calculate the Mössbauer properties we employed DFT to determine the parameters such as isomer shift (δ) and quadruple splitting (ΔE_Q) in ORCA 3.0.3. For this B3LYP functional with TZVP basis set was used and particularly for Fe, CP(PPP) (core properties basis set) was used. Also COSMO (Methanol) keywords were used to incorporate the solvent effect. Mossbauer parameters are calculated using the linear equation $\delta = \alpha(\rho - c) + \beta$.¹ The wave function for use in quantum theory of atoms in molecules (QTAIM) analysis were generated from single point calculation using hybrid B3LYP functional with TZV Ahlrichs triple- ζ basis set as implemented in the Gaussian 09 suite (Revision A.02) of programs.² Further, the quantum theory of atoms in molecule (QTAIM) was applied to depict the topological properties of the chosen complexes. To better understand the nature of the coordination of the complexes to explain the variation of E/D and consistency of D values we have used the Baders Atoms in Molecules theory.³ In this theory, Bader and co-workers characterizes bonding and non-bonding interactions of atoms in terms of topological

SUPPORTING INFORMATION

properties such as electron density $\rho(r)$, Laplacian of the electron density $L(r)$, potential energy density $V(r)$, kinetic energy density $G(r)$, total energy density $H(r)$ and a potential energy to the Lagrangian kinetic energy ratio ($|V(r)/G(r)|$). For instance, the presence of a (3, -1) critical point in QTAIM topography represents a chemical bond between two atoms and are called as the bond critical points (BCPs) where the shared electron density reaches a minimum, whereas a critical point with (3, +1) and (3, +3) signatures identify a ring structure (RCP) and cage critical point (CCP) in the molecular system. The $\rho(r)$ values at the BCPs are related to the strength of the bonds.⁴ In this study, QTAIM calculations are performed at B3LYP/TZV level using AIM2000 package.⁵

Table S1: Continuous shape analysis (CShMs).⁶

Dihedral angle (θ_d)	Tetrahedron	Square Planar
89.98°	2.065	27.838
81.38°	2.073	23.632
72.41°	3.513	18.821
59.9°	6.097	13.275
49.8°	9.143	9.362
39.7°	12.948	6.063
30.7°	16.952	3.674
20.8°	21.895	1.744
11.0°	27.305	0.559
2.6°	33.123	0.139

SUPPORTING INFORMATION

Table S2. Topological parameters at BCPs in the Fe–S bonds of the chosen complexes. All parameters are in a.u. $\rho(r)$ in units of $e\text{\AA}^{-3}$, G(r), V(r), H(r) in units of a.u.

Dihedral (θ_d)	Fe–S ₁ bonds							Fe–S ₂ bonds							
	$\rho(r)$	$\nabla_{\rho(r)}^2$	H(r)	G(r)	ε	V(r)	V(r) /G(r)	$\rho(r)$	$\nabla_{\rho(r)}^2$	H(r)	G(r)	ε	V(r)	V(r) /G(r)	
89.98°	0.0642	0.0412	-0.0161	0.0573	0.1670	0.0734	1.2812	0.0643	0.0406	-0.0163	0.0569	0.1507	0.0733	1.2870	
81.38°	0.0644	0.0403	-0.0164	0.0567	0.1489	0.0730	1.2891	0.0663	0.0418	-0.0174	0.0592	0.1483	0.0765	1.2934	
72.41°	0.0654	0.0417	-0.0168	0.0585	0.1752	0.0753	1.2875	0.0648	0.0408	-0.0167	0.0575	0.1544	0.0743	1.2904	
80.00°	0.0641	0.0408	-0.0162	0.0570	0.1684	0.0732	1.2840	0.0642	0.0409	-0.0162	0.0571	0.1680	0.0734	1.2839	
69.90°	0.0643	0.0405	-0.0164	0.0569	0.1578	0.0732	1.2880	0.0645	0.0404	-0.0165	0.0569	0.1465	0.0734	1.2901	
59.90°	0.0647	0.0396	-0.0167	0.0564	0.1295	0.0731	1.2968	0.0650	0.0394	-0.0170	0.0564	0.1086	0.0733	1.3010	
49.80°	0.0654	0.0384	-0.0173	0.0557	0.0903	0.0729	1.3101	0.0657	0.0380	-0.0176	0.0556	0.0640	0.0732	1.3158	
39.70°	0.0662	0.0370	-0.0179	0.0549	0.0601	0.0728	1.3260	0.0665	0.0366	-0.0182	0.0548	0.0337	0.0730	1.3323	
30.70°	0.0682	0.0318	-0.0196	0.0514	0.3236	0.0710	1.3813	0.0682	0.0323	-0.0197	0.0520	0.3467	0.0718	1.3808	
20.80°	0.0686	0.0312	-0.0200	0.0512	0.4670	0.0712	1.3906	0.0685	0.0310	-0.0200	0.0510	0.4554	0.0710	1.3922	
11.00°	0.0684	0.0322	-0.0201	0.0523	0.3874	0.0724	1.3843	0.0679	0.0333	-0.0199	0.0532	0.3027	0.07311	1.3742	
2.6°	0.0684	0.0326	-0.0202	0.0528	0.3468	0.0730	1.3826	0.0683	0.0324	-0.0201	0.0525	0.3368	0.0727	1.3848	
62.70°	0.0646	0.0399	-0.0166	0.0565	0.1388	0.0731	1.2937	0.0649	0.0398	-0.0168	0.0566	0.1211	0.0735	1.2975	
64.70°	0.0645	0.0401	-0.0165	0.0566	0.1448	0.0732	1.2920	0.0647	0.0399	-0.0167	0.0566	0.1288	0.0733	1.2950	
67.40°	0.0644	0.0403	-0.0164	0.0568	0.1521	0.0732	1.2898	0.0645	0.0401	-0.0165	0.0567	0.1384	0.0732	1.2921	
		Fe–S ₃ bonds							Fe–S ₄ bonds						
		$\rho(r)$	$\nabla_{\rho(r)}^2$	H(r)	G(r)	ε	V(r)	V(r) /G(r)	$\rho(r)$	$\nabla_{\rho(r)}^2$	H(r)	G(r)	ε	V(r)	V(r) /G(r)
89.98°	0.0642	0.0409	-0.0162	0.0571	0.1664	0.0733	1.2840	0.0641	0.0411	-0.0161	0.0572	0.1759	0.0733	1.2816	
81.38°	0.0660	0.0426	-0.0172	0.0598	0.1893	0.0770	1.2874	0.0651	0.0423	-0.0166	0.0589	0.2061	0.0756	1.2819	
72.41°	0.0638	0.0393	-0.0163	0.0556	0.1215	0.0719	1.2930	0.0653	0.0411	-0.0167	0.0578	0.1469	0.0746	1.2890	
80.00°	0.0643	0.0405	-0.0164	0.0569	0.1489	0.0733	1.2881	0.0643	0.0411	-0.0162	0.0572	0.1626	0.0734	1.2825	
69.90°	0.0646	0.0400	-0.0166	0.0567	0.1342	0.0733	1.2934	0.0645	0.0407	-0.0164	0.0570	0.1477	0.0734	1.2874	
59.90°	0.0651	0.0391	-0.0170	0.0562	0.1018	0.0732	1.3034	0.0650	0.0398	-0.0168	0.0566	0.1195	0.0734	1.2968	
49.80°	0.0657	0.0379	-0.0176	0.0554	0.0605	0.0730	1.3172	0.0656	0.0385	-0.0173	0.0559	0.0865	0.0732	1.3102	
39.70°	0.0665	0.0364	-0.0182	0.0546	0.0292	0.0728	1.3331	0.0664	0.0371	-0.0180	0.0551	0.0629	0.0730	1.3262	
30.70°	0.0676	0.0329	-0.0196	0.0524	0.3153	0.0720	1.3740	0.0677	0.0327	-0.0194	0.0521	0.3387	0.0715	1.3723	
20.80°	0.0671	0.0353	-0.0194	0.0547	0.2390	0.0740	1.3528	0.0669	0.0354	-0.0193	0.0547	0.2299	0.0740	1.3528	
11.00°	0.0676	0.0339	-0.0198	0.0536	0.3052	0.0734	1.3694	0.0683	0.0323	-0.0200	0.0523	0.3702	0.0724	1.3843	

SUPPORTING INFORMATION

2.6°	0.0679	0.0334	-0.0199	0.0533	0.3380	0.0732	1.3734	0.0681	0.0332	-0.0200	0.0532	0.3380	0.0733	1.3778
62.70°	0.0649	0.0398	-0.0168	0.0566	0.1211	0.0735	1.2975	0.0649	0.0394	-0.0169	0.0563	0.1127	0.0732	1.3000
64.70°	0.0648	0.0396	-0.0168	0.0564	0.1200	0.0732	1.2978	0.0648	0.0403	-0.0166	0.0568	0.1344	0.0734	1.2918
67.40°	0.0647	0.0398	-0.0167	0.0566	0.1274	0.0733	1.2954	0.0646	0.0405	-0.0165	0.0569	0.1412	0.0734	1.2895

Table S3. Topological parameters at BCPs in the Fe–S bonds of the chosen complexes. All parameters are in a.u. $\rho(r)$ in units of $e\text{\AA}^{-3}$, G(r), V(r), H(r) in units of a.u. (d = Avg. Fe-S bond length in \AA)

	Fe–S ₁ bonds							Fe–S ₂ bonds						
	$\rho(r)$	$\nabla_{\rho(r)}^2$	H(r)	G(r)	ϵ	V(r)	V(r) /G(r)	$\rho(r)$	$\nabla_{\rho(r)}^2$	H(r)	G(r)	ϵ	V(r)	V(r) /G(r)
$\theta_d = 90^\circ$, $d = 2.40$	0.0585	0.0370	-0.0133	0.0503	0.1812	0.0636	1.2644	0.0586	0.0365	-0.0135	0.0500	0.1646	0.0635	1.2700
$\theta_d = 90^\circ$, $d = 2.45$	0.0534	0.0332	-0.0109	0.0441	0.1939	0.0551	1.2482	0.0534	0.0327	-0.0111	0.0438	0.1773	0.0550	1.2538
$\theta_d = 90^\circ$, $d = 2.30$	0.0706	0.0459	-0.0194	0.0653	0.1526	0.0847	1.2978	0.0706	0.0452	-0.0197	0.0649	0.1368	0.0846	1.3036
$\theta_d = 90^\circ$, $d = 2.25$	0.0776	0.0510	-0.0234	0.0744	0.1361	0.0978	1.3147	0.0776	0.0502	-0.0237	0.0739	0.1211	0.0976	1.3204
$\theta_d = 30^\circ$, $d = 2.40$	0.0590	0.0383	-0.0144	0.0528	0.3173	0.0672	1.2737	0.0588	0.0382	-0.0142	0.0524	0.2812	0.0666	1.2712
$\theta_d = 30^\circ$, $d = 2.45$	0.0560	0.0282	-0.0129	0.0411	0.0508	0.0540	1.3140	0.0558	0.0284	-0.0127	0.0411	0.0640	0.0538	1.3086
$\theta_d = 30^\circ$, $d = 2.30$	0.0731	0.0419	-0.0221	0.0641	0.1322	0.0862	1.3455	0.0725	0.0421	-0.0216	0.0637	0.1567	0.0853	1.3394
$\theta_d = 30^\circ$, $d = 2.25$	0.0788	0.0522	-0.0254	0.0776	0.2609	0.1030	1.3276	0.0782	0.0523	-0.0248	0.0771	0.2553	0.1020	1.3220
$\theta_d = 40^\circ$, $d = 2.40$	0.0589	0.0380	-0.0142	0.0522	0.3339	0.0664	1.2718	0.0586	0.0377	-0.0140	0.0517	0.2782	0.0656	1.2702
$\theta_d = 40^\circ$, $d = 2.45$	0.0536	0.0343	-0.0117	0.0460	0.3547	0.0576	1.2536	0.0534	0.0339	-0.0115	0.0454	0.2739	0.0569	1.2533
$\theta_d = 40^\circ$, $d = 2.30$	0.0726	0.0420	-0.0217	0.0637	0.0481	0.0853	1.3403	0.0722	0.0423	-0.0213	0.0636	0.0712	0.0848	1.3343

SUPPORTING INFORMATION

$\theta_d = 40,$ $d = 2.25$	0.0781	0.0531	-0.0247	0.0778	0.2762	0.1025	1.3176	0.0775	0.0531	-0.0240	0.0771	0.2417	0.1012	1.3115
$\theta_d = 50,$ $d = 2.40$	0.0601	0.0336	-0.0146	0.0482	0.0548	0.0629	1.3035	0.0598	0.0339	-0.0144	0.0483	0.0835	0.0627	1.2976
$\theta_d = 50,$ $d = 2.45$	0.0535	0.0337	-0.0115	0.0451	0.3766	0.0566	1.2540	0.0534	0.0330	-0.0114	0.0444	0.2928	0.0557	1.2558
$\theta_d = 50,$ $d = 2.30$	0.0717	0.0440	-0.0208	0.0648	0.1092	0.0857	1.3213	0.0713	0.0442	-0.0205	0.0647	0.1213	0.0852	1.3167
$\theta_d = 50,$ $d = 2.25$	0.0780	0.0518	-0.0244	0.0763	0.2061	0.1007	1.3205	0.0777	0.0516	-0.0241	0.0757	0.1747	0.0998	1.3180
$\theta_d = 60,$ $d = 2.40$	0.0594	0.0348	-0.0141	0.0489	0.0913	0.0630	1.2891	0.0592	0.0351	-0.0139	0.0490	0.1194	0.0629	1.2844
$\theta_d = 60,$ $d = 2.45$	0.0543	0.0308	-0.0117	0.0426	0.0852	0.0543	1.2751	0.0541	0.0311	-0.0115	0.0427	0.1158	0.0542	1.2702
$\theta_d = 60,$ $d = 2.30$	0.0711	0.0451	-0.0202	0.0653	0.1456	0.0855	1.3095	0.0708	0.0452	-0.0200	0.0651	0.1476	0.0851	1.3065
$\theta_d = 60,$ $d = 2.25$	0.0778	0.0512	-0.0241	0.0753	0.1727	0.0994	1.3199	0.0776	0.0510	-0.0238	0.0749	0.1519	0.0987	1.3180
$\theta_d = 70,$ $d = 2.40$	0.0589	0.0358	-0.0137	0.0495	0.1336	0.0632	1.2771	0.0587	0.0360	-0.0136	0.0496	0.1563	0.0632	1.2742
$\theta_d = 70,$ $d = 2.45$	0.0538	0.0318	-0.0113	0.0432	0.1259	0.0545	1.2630	0.0536	0.0320	-0.0112	0.0433	0.1549	0.0545	1.2598
$\theta_d = 70,$ $d = 2.30$	0.0707	0.0455	-0.0198	0.0653	0.1569	0.0851	1.3033	0.0705	0.0454	-0.0197	0.0651	0.1533	0.0848	1.3020
$\theta_d = 70,$ $d = 2.25$	0.0776	0.0510	-0.0237	0.0747	0.1580	0.0985	1.3177	0.0774	0.0508	-0.0236	0.0744	0.1421	0.0980	1.3170
$\theta_d = 80,$ $d = 2.40$	0.0585	0.0366	-0.0134	0.0500	0.1703	0.0634	1.2686	0.0585	0.0366	-0.0134	0.0500	0.1799	0.0634	1.2682
$\theta_d = 80,$ $d = 2.45$	0.0534	0.0326	-0.0111	0.0437	0.1692	0.0548	1.2535	0.0533	0.0327	-0.0111	0.0437	0.1880	0.0548	1.2527
$\theta_d = 80,$ $d = 2.30$	0.0705	0.0457	-0.0195	0.0652	0.1605	0.0848	1.2996	0.0704	0.0455	-0.0195	0.0650	0.1536	0.0846	1.3002
$\theta_d = 80,$	0.0775	0.0509	-0.0235	0.0744	0.1499	0.0979	1.3158	0.0774	0.0507	-0.0235	0.0741	0.1376	0.0976	1.3166

SUPPORTING INFORMATION

d = 2.25																
	Fe–S ₃ bonds							Fe–S ₄ bonds								
	$\rho(r)$	$\nabla_{\rho(r)}^2$	H(r)	G(r)	ε	V(r)	V(r) /G(r)	$\rho(r)$	$\nabla_{\rho(r)}^2$	H(r)	G(r)	ε	V(r)	V(r) /G(r)		
$\theta_d = 90,$ $d = 2.40$	0.0584	0.0366	-0.0134	0.0500	0.1792	0.0634	1.2680	0.0584	0.0369	-0.0133	0.0502	0.1891	0.0635	1.2651		
$\theta_d = 90,$ $d = 2.45$	0.0533	0.0329	-0.0110	0.0439	0.1918	0.0549	1.2510	0.0532	0.0331	-0.0109	0.0440	0.2022	0.0550	1.2486		
$\theta_d = 90,$ $d = 2.30$	0.0704	0.0455	-0.0195	0.0650	0.1519	0.0845	1.3005	0.0704	0.0457	-0.0194	0.0652	0.1610	0.0846	1.2981		
$\theta_d = 90,$ $d = 2.25$	0.0774	0.0506	-0.0235	0.0741	0.1367	0.0975	1.3172	0.0774	0.0509	-0.0234	0.0742	0.1453	0.0976	1.3147		
$\theta_d = 30,$ $d = 2.40$	0.0591	0.0384	-0.0143	0.0528	0.2929	0.0671	1.2717	0.0590	0.0379	-0.0145	0.0523	0.2841	0.0668	1.2764		
$\theta_d = 30,$ $d = 2.45$	0.0560	0.0286	-0.0128	0.0414	0.0668	0.0542	1.3081	0.0560	0.0281	-0.0129	0.0410	0.0490	0.0540	1.3148		
$\theta_d = 30,$ $d = 2.30$	0.0730	0.0425	-0.0219	0.0644	0.1557	0.0863	1.3399	0.0728	0.0418	-0.0220	0.0637	0.1401	0.0857	1.3446		
$\theta_d = 30,$ $d = 2.25$	0.0787	0.0526	-0.0252	0.0778	0.2674	0.1030	1.3238	0.0784	0.0521	-0.0252	0.0773	0.2617	0.1025	1.3259		
$\theta_d = 40,$ $d = 2.40$	0.0589	0.0383	-0.0140	0.0523	0.3398	0.0664	1.2684	0.0588	0.0376	-0.0142	0.0518	0.2872	0.0659	1.2740		
$\theta_d = 40,$ $d = 2.45$	0.0536	0.0345	-0.0115	0.0460	0.3539	0.0576	1.2506	0.0536	0.0338	-0.0117	0.0455	0.2864	0.0572	1.2571		
$\theta_d = 40,$ $d = 2.30$	0.0725	0.0425	-0.0214	0.0640	0.0664	0.0854	1.3348	0.0726	0.0418	-0.0217	0.0635	0.0466	0.0851	1.3415		
$\theta_d = 40,$ $d = 2.25$	0.0713	0.0474	-0.0208	0.0682	0.2519	0.0889	1.3044	0.0781	0.0520	-0.0247	0.0767	0.2267	0.1014	1.3225		
$\theta_d = 50,$ $d = 2.40$	0.0600	0.0341	-0.0144	0.0485	0.0849	0.0630	1.2975	0.0601	0.0335	-0.0147	0.0482	0.0505	0.0628	1.3048		
$\theta_d = 50,$ $d = 2.45$	0.0535	0.0339	-0.0113	0.0453	0.3895	0.0566	1.2505	0.0535	0.0330	-0.0115	0.0445	0.2907	0.0560	1.2592		
$\theta_d = 50,$ $d = 2.30$	0.0717	0.0444	-0.0206	0.0650	0.1101	0.0857	1.3171	0.0717	0.0436	-0.0209	0.0645	0.1010	0.0854	1.3238		

SUPPORTING INFORMATION

$\theta_d = 50$, $d = 2.25$	0.0781	0.0520	-0.0243	0.0763	0.1799	0.1005	1.3180	0.0780	0.0512	-0.0245	0.0756	0.1754	0.1001	1.3237
$\theta_d = 60$, $d = 2.40$	0.0594	0.0352	-0.0140	0.0492	0.1139	0.0632	1.2843	0.0595	0.0346	-0.0142	0.0488	0.0874	0.0630	1.2911
$\theta_d = 60$, $d = 2.45$	0.0543	0.0313	-0.0116	0.0428	0.1137	0.0544	1.2699	0.0544	0.0308	-0.0118	0.0425	0.0814	0.0543	1.2769
$\theta_d = 60$, $d = 2.30$	0.0711	0.0454	-0.0201	0.0654	0.1377	0.0855	1.3066	0.0711	0.0446	-0.0203	0.0650	0.1288	0.0853	1.3129
$\theta_d = 60$, $d = 2.25$	0.0779	0.0514	-0.0239	0.0753	0.1523	0.0993	1.3178	0.0779	0.0506	-0.0242	0.0748	0.1438	0.0989	1.3236
$\theta_d = 70$, $d = 2.40$	0.0589	0.0361	-0.0136	0.0498	0.1460	0.0634	1.2737	0.0590	0.0356	-0.0138	0.0494	0.1281	0.0633	1.2797
$\theta_d = 70$, $d = 2.45$	0.0538	0.0322	-0.0112	0.0434	0.1462	0.0546	1.2591	0.0539	0.0317	-0.0114	0.0431	0.1233	0.0546	1.2653
$\theta_d = 70$, $d = 2.30$	0.0708	0.0457	-0.0197	0.0654	0.1482	0.0852	1.3013	0.0708	0.0450	-0.0200	0.0650	0.1360	0.0849	1.3072
$\theta_d = 70$, $d = 2.25$	0.0778	0.0511	-0.0237	0.0748	0.1430	0.0985	1.3163	0.0777	0.0504	-0.0239	0.0743	0.1297	0.0982	1.3219
$\theta_d = 80$, $d = 2.40$	0.0586	0.0368	-0.0134	0.0502	0.1707	0.0635	1.2669	0.0587	0.0363	-0.0136	0.0499	0.1577	0.0634	1.2725
$\theta_d = 80$, $d = 2.45$	0.0535	0.0328	-0.0110	0.0439	0.1760	0.0549	1.2514	0.0535	0.0324	-0.0112	0.0436	0.1624	0.0548	1.2569
$\theta_d = 80$, $d = 2.30$	0.0706	0.0458	-0.0195	0.0654	0.1519	0.0849	1.2986	0.0706	0.0452	-0.0198	0.0649	0.1370	0.0847	1.3043
$\theta_d = 80$, $d = 2.25$	0.0776	0.0510	-0.0235	0.0745	0.1384	0.0980	1.3151	0.0776	0.0503	-0.0237	0.0740	0.1226	0.0977	1.3206

SUPPORTING INFORMATION

Table S4: NEVPT2 transition energy of the ligand field states and their individual contribution to the D and E values (only upto ^3H shown).

Complex 1 [Fe(C ₃ S ₅) ₂] ²⁻			NEVPT2 energy levels	Effective Hamiltonian Approach	
States			Energy (cm ⁻¹)	Contribution to D (cm ⁻¹)	Contribution to E (cm ⁻¹)
^5D	^5E	$^5\text{A}_1$	000.0	0.000	0.000
		$^5\text{B}_1$	2133.2	0.023	-0.009
	$^5\text{T}_2$	$^5\text{B}_2$	2261.3	0.005	0.003
		^5E	7407.6	1.973	1.656
			7460.1	1.908	-1.589
^3H	$^3\text{T}_1$	^3E	16029.5	-0.633	-0.392
			16038.2	-0.647	0.417
		$^3\text{A}_2$	16665.8	0.010	-0.006
	$^3\text{T}_2$	$^3\text{B}_2$	16683.0	-0.014	0.013
			20520.8	4.909	0.000
		^3E	21641.5	0.075	-0.008
	^3E	$^3\text{A}_1$	21690.3	0.192	0.000
		$^3\text{B}_1$	21781.3	-0.008	0.008
	$^3\text{T}_1$	^3E	22366.9	0.000	0.000
			22589.2	0.000	0.000
		$^3\text{A}_2$	23031.6	-0.003	0.001
				Overall D = 6.122	Overall E = 0.09

SUPPORTING INFORMATION

Table S5: Major electronic configurations arising from the first five quintet states

SA-CASSCF states of Complex 1	Major Electronic configurations (%)	Contribution to D (NEVPT2/EHA) (cm ⁻¹)	Contribution to E (NEVPT2/EHA) (cm ⁻¹)
Ground state (⁵ A ₁)	d _{z2} ² d _{x2-y2} ¹ d _{xy} ¹ d _{xz} ¹ d _{yz} ¹ (100%)	0.000	0.000
1 st excited state (⁵ B ₁)	d _{z2} ¹ d _{x2-y2} ² d _{xy} ¹ d _{xz} ¹ d _{yz} ¹ (74%)	0.023	-0.009
2 nd excited state (⁵ B ₁)	d _{z2} ¹ d _{x2-y2} ¹ d _{xy} ² d _{xz} ¹ d _{yz} ¹ (75%)	0.005	0.003
3 rd excited state (⁵ E)	d _{z2} ¹ d _{x2-y2} ¹ d _{xy} ¹ d _{xz} ² d _{yz} ¹ (97%)	1.973	1.656
4 th excited state (⁵ E)	d _{z2} ¹ d _{x2-y2} ¹ d _{xy} ¹ d _{xz} ¹ d _{yz} ² (97%)	1.908	-1.589

Table S6: NEVPT2 transition energy of the ligand field states and their individual contribution to the D and E values (only upto ³H shown).

Complex 2 [Fe(C ₃ S ₅) ₂] ²⁻			NEVPT2 energy levels	Effective Hamiltonian Approach	
States			Energy (cm ⁻¹)	Contribution to D (cm ⁻¹)	Contribution to E (cm ⁻¹)
⁵ D	⁵ E	⁵ A ₁	000.0	0.000	0.000
		⁵ B ₁	2258.7	-0.001	0.020
	⁵ T ₂	⁵ B ₂	2655.4	0.032	-0.012
		⁵ E	6521.6	2.249	2.080
			8434.0	1.659	-1.472
³ H	³ T ₁	³ E	15633.1	-0.177	0.164
		³ A ₂	16222.2	-0.079	-0.060
		³ A ₁	16641.4	-0.527	-0.436
	³ T ₂	³ B ₂	17314.5	-0.466	0.424
		³ E	20708.5	0.494	0.000
		³ E	20889.8	-0.002	0.005
	³ E	³ A ₁	21052.5	4.262	0.001
		³ B ₁	21681.4	0.007	-0.001
	³ T ₁	³ E	22606.4	0.000	0.000
		³ E	23016.5	0.004	0.000
		³ A ₂	23492.4	0.001	0.000
				Overall D = 6.067	Overall E = 0.67

SUPPORTING INFORMATION

Table S7: NEVPT2 transition energy of the ligand field states and their individual contribution to the D and E values (only upto ${}^3\text{H}$ shown).

Complex 3 [Fe(C ₃ S ₅) ₂] ²⁻			NEVPT2 energy levels	Effective Hamiltonian Approach	
States			Energy (cm ⁻¹)	Contribution to D (cm ⁻¹)	Contribution to E (cm ⁻¹)
${}^5\text{D}$	${}^5\text{E}$	${}^5\text{A}_1$	000.0	0.000	0.000
		${}^5\text{B}_1$	1915.3	0.014	-0.026
	${}^5\text{T}_2$	${}^5\text{B}_2$	2198.8	-0.041	0.025
		${}^5\text{E}$	5664.2	2.731	2.727
			9579.8	1.377	-1.368
${}^3\text{H}$	${}^3\text{T}_1$	${}^3\text{E}$	14038.1	-0.361	0.365
			14180.1	-0.225	-0.255
		${}^3\text{A}_2$	17587.9	-0.115	-0.242
	${}^3\text{T}_2$	${}^3\text{B}_2$	18051.7	0.085	-0.021
		${}^3\text{E}$	18668.5	-0.288	0.287
			20497.9	-0.087	0.086
	${}^3\text{E}$	${}^3\text{A}_1$	21236.8	0.240	-0.015
		${}^3\text{B}_1$	21318.9	3.472	-0.003
	${}^3\text{T}_1$	${}^3\text{E}$	22452.6	-0.005	0.005
			22664.5	-0.004	0.001
		${}^3\text{A}_2$	23658.2	0.164	-0.002
				Overall D = 6.014	Overall E = 1.45

SUPPORTING INFORMATION

Table S8: NEVPT2 transition energy of the ligand field states and their individual contribution to the D and E values (only upto ${}^3\text{H}$ shown).

$\theta_d = 60^\circ$ $[\text{Fe}(\text{C}_3\text{S}_5)_2]^{2-}$		NEVPT2 energy levels	Effective Hamiltonian Approach	
States		Energy (cm^{-1})	Contribution to D (cm^{-1})	Contribution to E (cm^{-1})
${}^5\text{D}$	${}^5\text{E}$	000.0	0	0
		1486.6	-0.117	-0.002
	${}^5\text{T}_2$	2084.0	0.14	0.181
		4545.0	-7.228	0.001
		10984.1	1.09	-1.09
${}^3\text{H}$	${}^3\text{T}_1$	12139.0	-0.626	0.624
		12386.4	0.738	-0.003
		15177.3	-0.132	-0.132
		18810.9	0.036	-0.002
	${}^3\text{T}_2$	19355.4	0.182	-0.016
		19427.0	-0.145	-0.147
		20885.9	-0.344	0.31
	${}^3\text{E}$	21590.5	-0.01	0.011
		22196.2	-0.26	-0.263
	${}^3\text{T}_1$	22256.0	-1.397	-1.4
		23416.9	0.002	-0.001
			Overall D = -7.32	Overall E = -1.58

SUPPORTING INFORMATION

Table S9: NEVPT2 transition energy of the ligand field states and their individual contribution to the D and E values (only upto ^3H shown).

$\theta_d = 50^\circ$ $[\text{Fe}(\text{C}_3\text{S}_5)_2]^{2-}$		NEVPT2 energy levels	Effective Hamiltonian Approach	
States		Energy (cm^{-1})	Contribution to D (cm^{-1})	Contribution to E (cm^{-1})
^5D	^5E	000.0	0.000	0.000
		1000.6	-0.187	-0.003
	$^5\text{T}_2$	1930.2	0.608	0.662
		3774.8	-9.424	0.007
		12171.6	0.776	-0.715
^3H	$^3\text{T}_1$	10450.7	-1.059	0.993
		10851.1	0.832	-0.001
	$^3\text{T}_2$	12990.9	-0.108	-0.107
		18283.4	0.000	0.000
	^3E	18843.2	-0.008	-0.045
		20205.3	-0.161	-0.151
	$^3\text{T}_1$	20331.7	-0.022	0.017
		21512.7	-0.311	0.245
		21923.3	-0.302	-0.281
		21951.0	0.000	0.001
		23181.8	-1.192	-1.092
			Overall D = -9.58	Overall E = -0.21

SUPPORTING INFORMATION

Table S10: NEVPT2 transition energy of the ligand field states and their individual contribution to the D and E values (only up to ^3H shown).

$\theta_d = 40^\circ$ [Fe(C ₃ S ₅) ₂] ²⁻		NEVPT2 energy levels	Effective Hamiltonian Approach	
States		Energy (cm ⁻¹)	Contribution to D (cm ⁻¹)	Contribution to E (cm ⁻¹)
^5D	^5E	000.0	0.000	0.000
		388.0	0.240	0.226
	$^5\text{T}_2$	1708.8	3.163	-2.768
		3088.4	6.082	5.879
		13375.5	-0.635	-0.001
^3H	$^3\text{T}_1$	8593.1	4.089	0.009
		9202.9	-0.347	-0.347
		10810.0	-0.027	0.024
	$^3\text{T}_2$	16573.6	0.000	0.000
		18728.7	-0.112	0.07
		19509.5	-0.164	0.161
	^3E	20571.5	0.646	0.000
		21280.3	-0.818	0.818
		21746.4	0.003	0.000
	$^3\text{T}_1$	21756.6	-0.009	0.013
		22628.5	-0.117	-0.028
			Overall D = ± 11.00	Overall E = 0.27

Analytical Equations:

The rhombic parameter E depends on the difference between the transverse components of the diagonalized D tensor.

$$D = D_{ZZ} - \frac{1}{2}(D_{XX} + D_{YY}); E = \frac{1}{2}(D_{XX} - D_{YY})$$

When the beta electron is in the d_{z2} orbital (or D is positive) then the spin-allowed equations are-

$$E \propto \frac{3}{2} \left[\frac{1}{E_{yz}} - \frac{1}{E_{xz}} \right]$$

$$D_{xx} = -\frac{\zeta^2 |\langle d_{z2} | \mathcal{L}_x | d_{yz} \rangle \langle d_{yz} | \mathcal{L}_y | d_{z2} \rangle|}{4S^2 (E_{yz} - E_{z2})}$$

$$D_{yy} = -\frac{\zeta^2 |\langle d_{z2} | \mathcal{L}_y | d_{zx} \rangle \langle d_{zx} | \mathcal{L}_y | d_{z2} \rangle|}{4S^2 (E_{zx} - E_{z2})}$$

SUPPORTING INFORMATION

$$D_{zz} = 0$$

When the beta electron is in the $d_{x^2-y^2}$ orbital (or D is negative) then the applicable spin-allowed equations are-

$$E \propto \frac{1}{2} \left[\frac{1}{E_{yz}} - \frac{1}{E_{xz}} \right]$$
$$D_{xx} = -\frac{\zeta^2 |\langle d_{x^2-y^2} | \hat{L}_x | d_{yz} \rangle \langle d_{yz} | \hat{L}_x | d_{x^2-y^2} \rangle|}{4S^2 \quad E_{yz} - E_{x^2-y^2}}$$

$$D_{yy} = -\frac{\zeta^2 |\langle d_{x^2-y^2} | \hat{L}_y | d_{xz} \rangle \langle d_{xz} | \hat{L}_y | d_{x^2-y^2} \rangle|}{4S^2 \quad E_{xz} - E_{x^2-y^2}}$$

$$D_{zz} = -\frac{\zeta^2 |\langle d_{x^2-y^2} | \hat{L}_z | d_{xy} \rangle \langle d_{xy} | \hat{L}_z | d_{x^2-y^2} \rangle|}{4S^2 \quad E_{xy} - E_{x^2-y^2}}$$

SUPPORTING INFORMATION

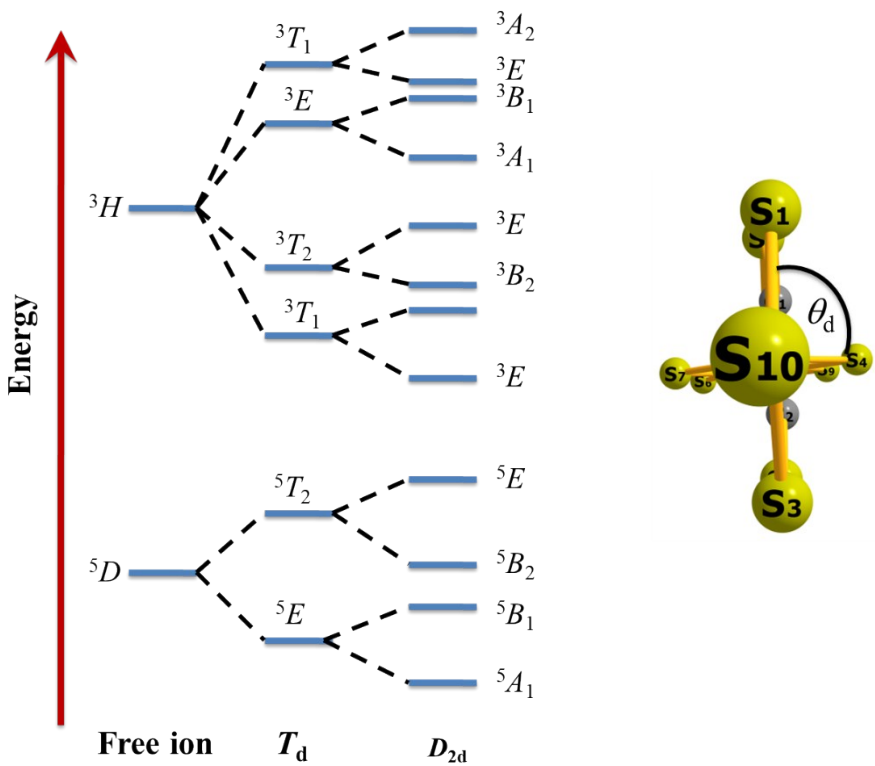
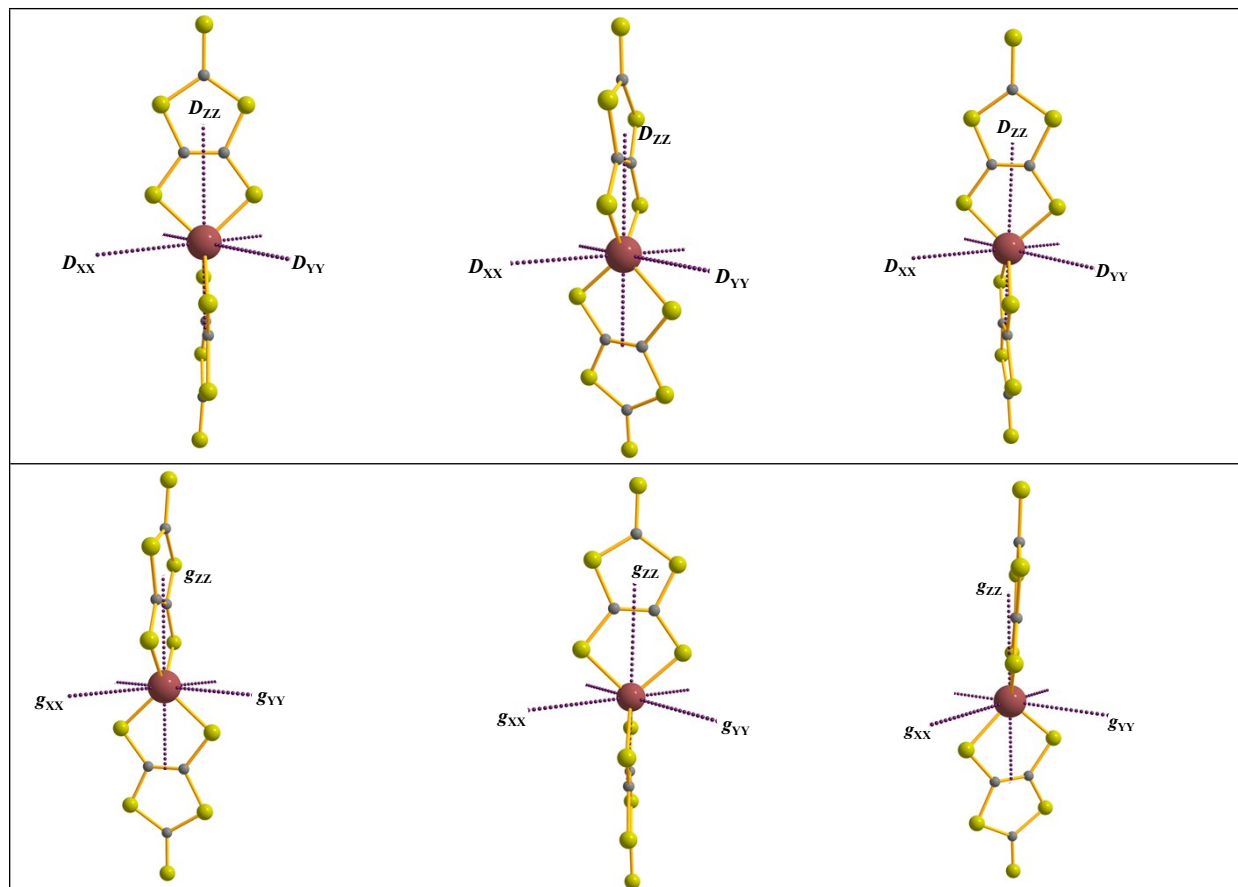


Fig. S1. Qualitative ligand field splitting diagram of a d^6 system in T_d followed by D_{2d} symmetry environment (left). Dihedral angle of the $[Fe(C_3S_5)_2]^{2-}$ moiety (right).



SUPPORTING INFORMATION

Fig S2. D & g orientations of original complexes- 1(left), 2(middle) & 3(right).

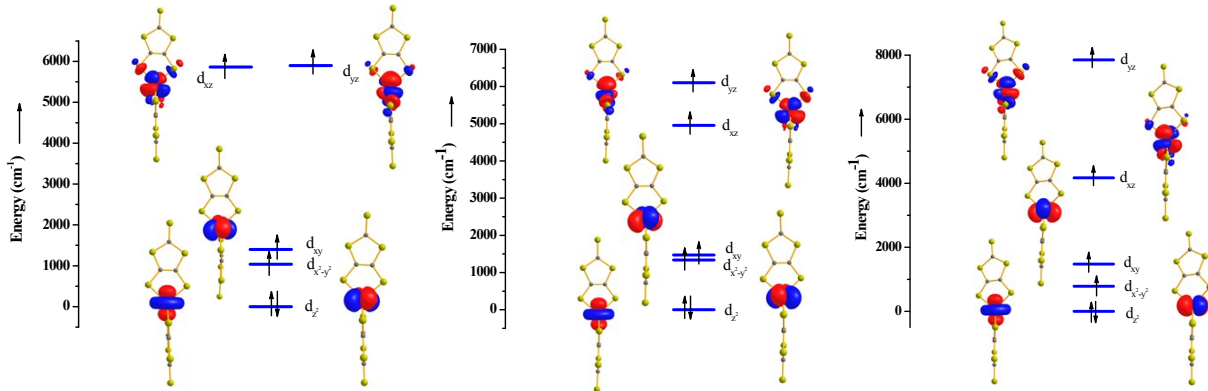


Fig. S3. d-orbital splitting of original complexes 1, 2 & 3.

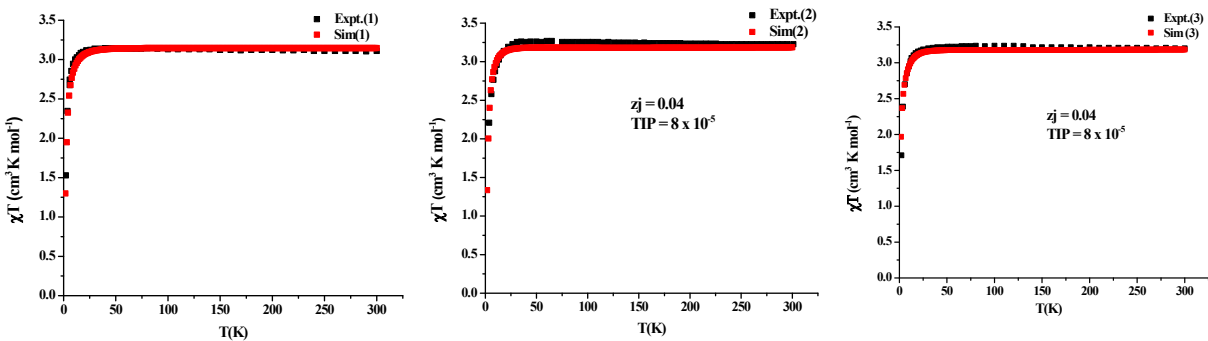
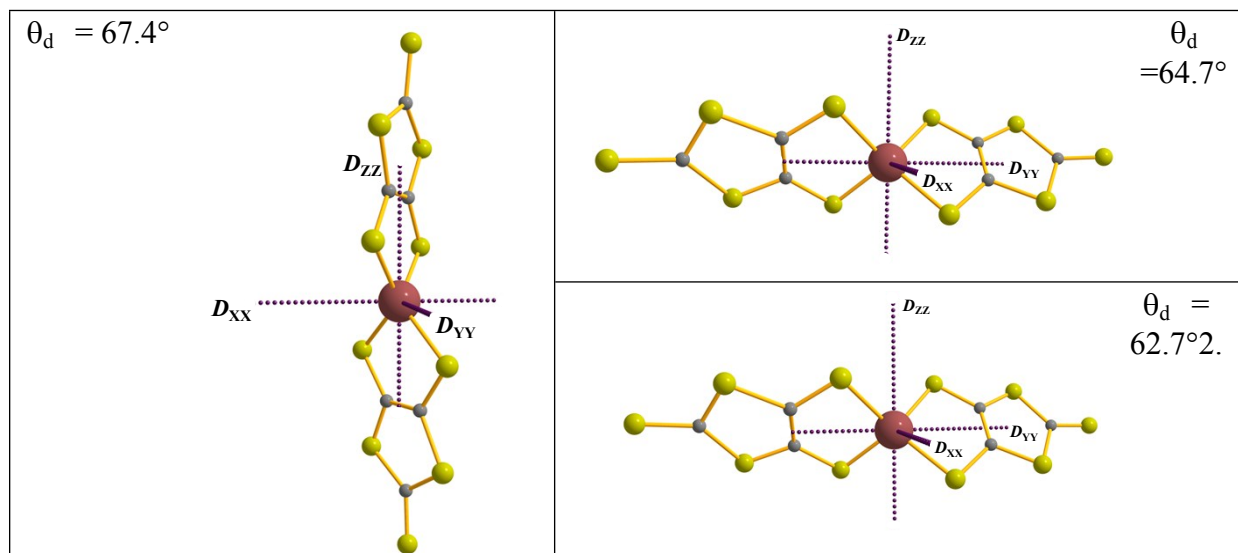


Figure S4. DC-magnetic susceptibility simulations along with the experimental points of the X-ray structures.



SUPPORTING INFORMATION

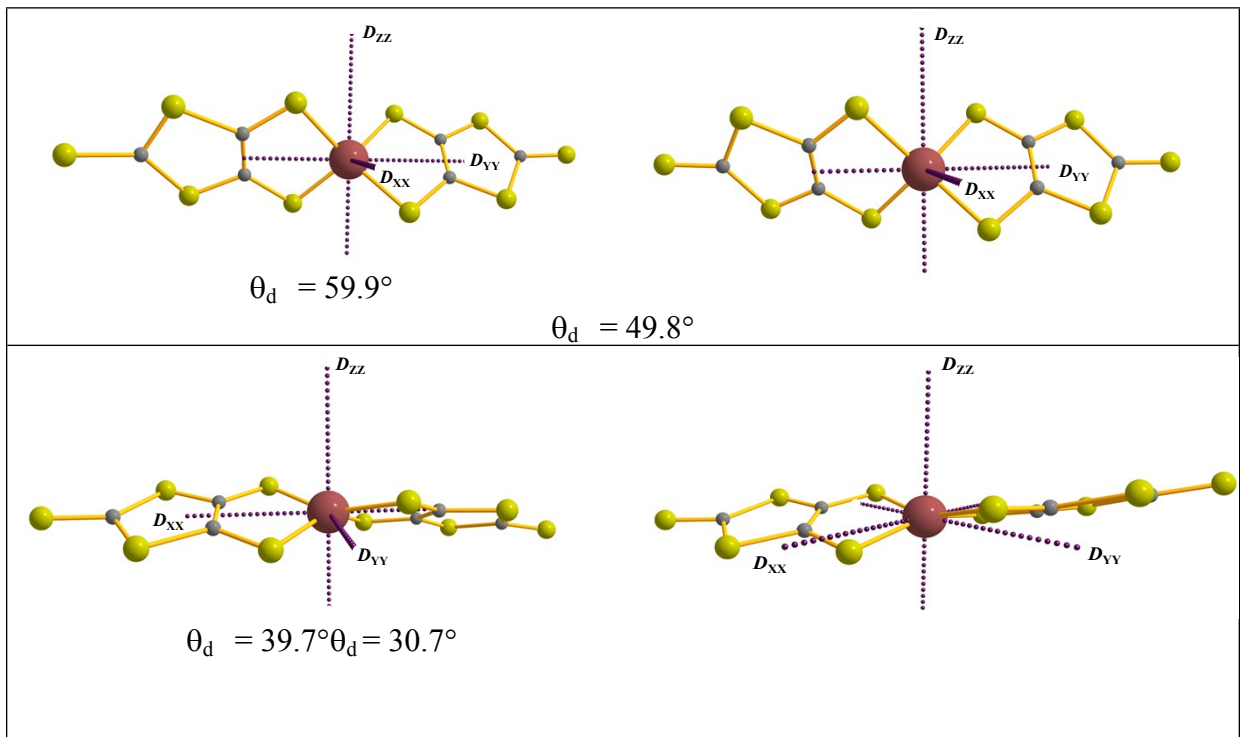
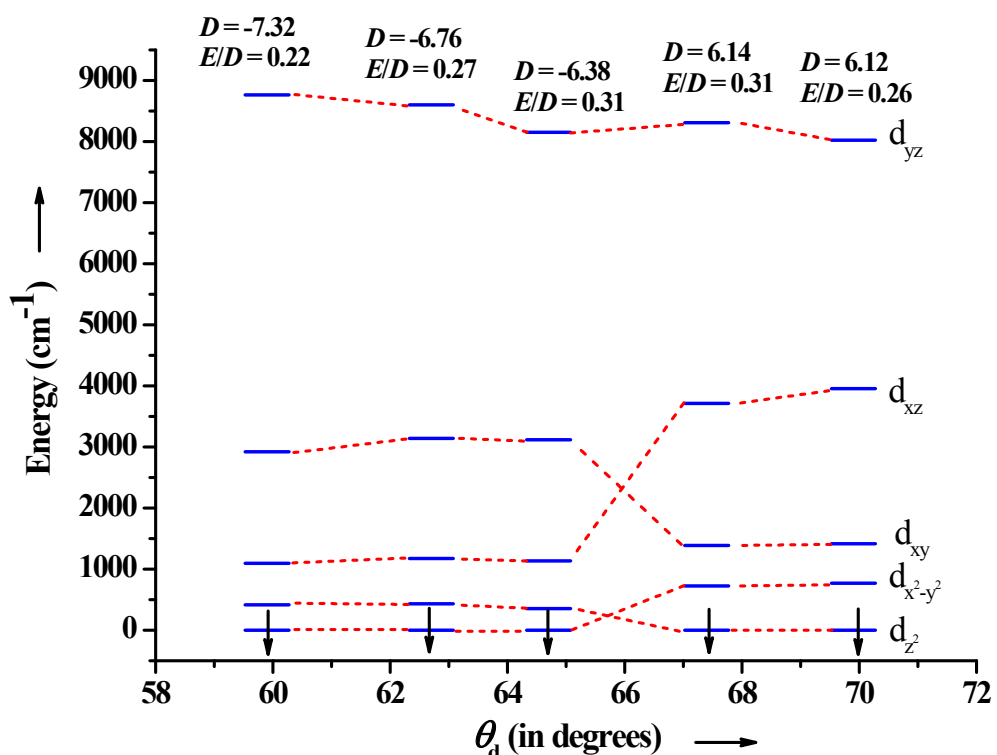


Fig. S5 D orientations of the model complexes. After the point $\theta_d = 30.7^\circ$ D orientation remains perpendicular to Fe-S₄ plane.



FigureS6: d-orbital splitting diagram from $\theta_d = 70^\circ$ to 60°

SUPPORTING INFORMATION

Table S11. NEVPT2 computed results of all the complexes with changing dihedral angle.

Dihedral angle (θ_d)	Roots (5, 45)		Roots (5, 45, 22)	
	D	E/D	D	E/D
89.98°	6.123	0.015	6.099	0.015
81.38°	6.067	0.111	6.039	0.118
72.41°	6.014	0.242	5.943	0.262
80.00°	6.124	0.117	6.093	0.127
69.90°	6.122	0.264	6.051	0.287
67.40°	6.136	0.310	-6.084	0.329
64.70°	-6.384	0.305	-6.566	0.275
62.70°	-6.758	0.267	-6.954	0.235
59.90°	-7.322	0.216	-7.535	0.182
49.80°	-9.584	0.022	-9.724	0.035
39.70°	-10.863	0.304	11.527	0.267
30.70°	16.064	0.040	16.393	0.042
20.80°	17.867	0.078	19.400	0.093
11.00°	18.515	0.090	20.171	0.098
2.6°	18.656	0.100	20.374	0.104

Table S12: Computed D parameter of θ_d from 90°-2° at different bond lengths (*values calculated considering CAS(10,7) active space including sulphur pi-bonding orbitals).

SUPPORTING INFORMATION

Avg. bond length (Å)	$\theta_d =$ 89.98°	80°	69.9°	59.9°	49.8°	39.7°	30.7°	20.8°	11.0°	2.6°
	D	D	D	D	D	D	D	D	D	D
2.25	4.90	4.83	4.54	4.33	3.92	3.72	-3.19	64.01*	56.82*	54.73*
2.30	5.50	5.48	5.40	5.50	-5.99	-8.07	-16.43	14.52*	113.63*	81.67*
2.35	6.12	6.12	6.12	-7.32	-9.58	-10.86	16.06	19.40	20.17	20.37
2.40	6.78	6.73	-7.20	-9.47	-11.32	12.92	15.65	18.67	20.49	18.79
2.45	7.51	7.33	-8.87	-11.18	-12.75	14.43	17.62	18.25	18.47	18.57

Table S13: Computed E/D parameter of θ_d from 90°-2° at different bond lengths (* values calculated considering CAS(10,7) active space including sulphur pi-bonding orbitals)

SUPPORTING INFORMATION

Avg. bond length (Å)	$\theta_d = 89.98^\circ$	80°	69.9°	59.9°	49.8°	39.7°	30.7°	20.8°	11.0°	2.6°
2.25	0.017	0.014	0.035	0.048	0.015	0.110	0.220	0.162*	0.102*	0.080*
2.30	0.015	0.060	0.150	0.250	0.290	0.106	0.164	0.205*	0.002*	0.053*
2.35	0.015	0.110	0.264	0.216	0.022	0.300	0.040	0.093	0.098	0.104
2.40	0.014	0.173	0.270	0.064	0.154	0.271	0.153	0.091	0.151	0.009
2.45	0.014	0.230	0.160	0.050	0.230	0.326	0.310	0.167	0.110	0.098

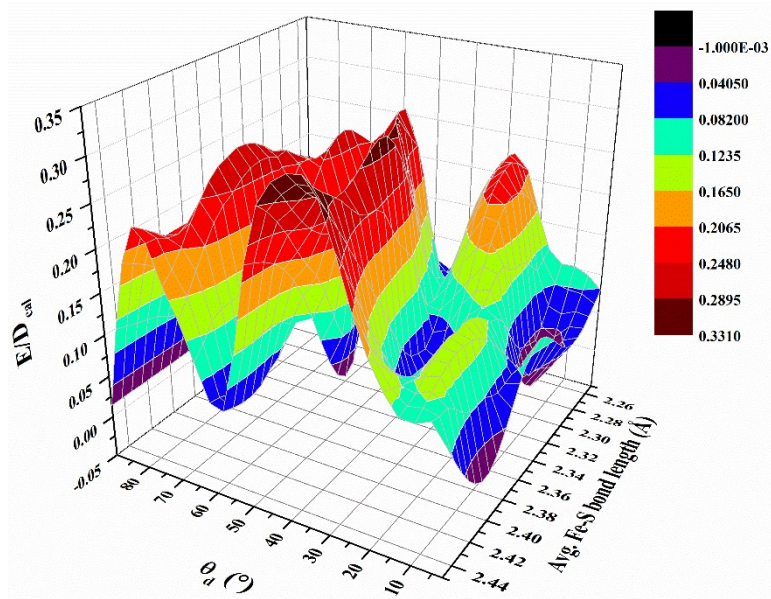


Figure S7. Three dimensional magneto-structural correlation developed between dihedral angle vs bond-length vs E/D parameter.

SUPPORTING INFORMATION

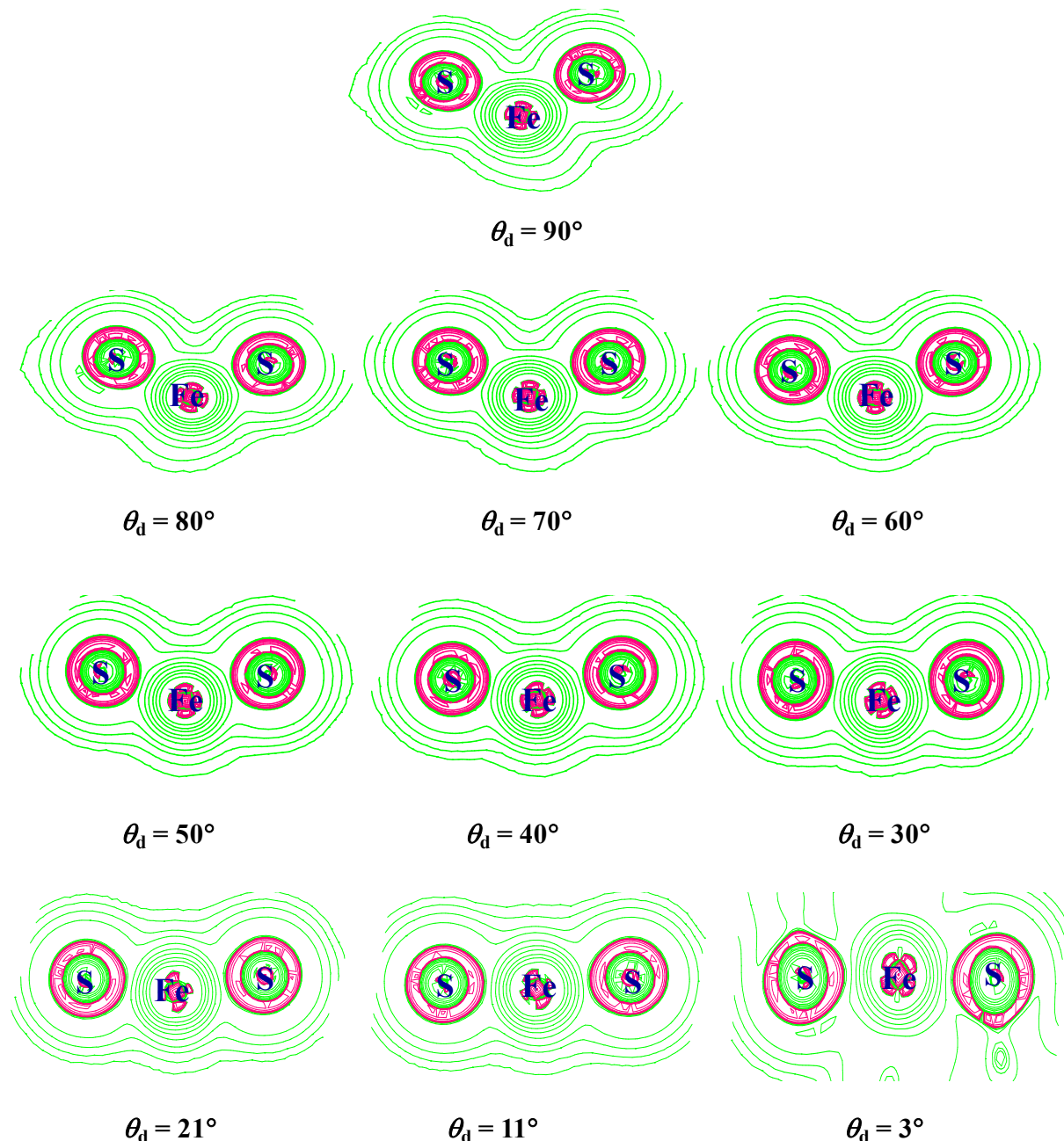


Fig. S8. Contour line diagram of the Laplacian of electron density along the Fe-S bond plane.

Solid green lines indicate charge depletion [$\nabla^2 \rho(r) > 0$] and solid pink lines indicate charge concentration [$\nabla^2 \rho(r) < 0$].

SUPPORTING INFORMATION

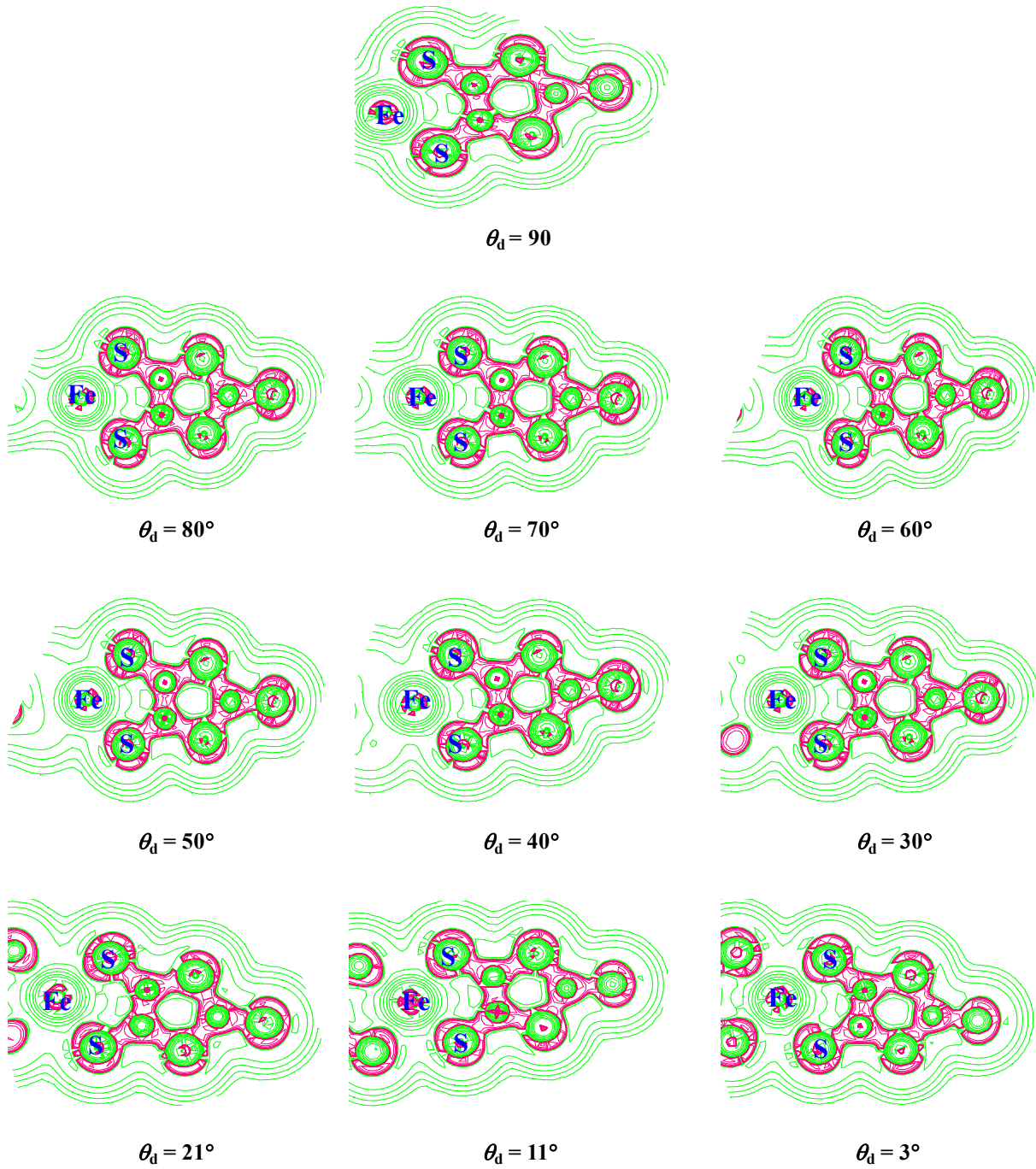


Fig. S9. Contour line diagram of the Laplacian of electron density along the Fe-ligand plane. Solid green lines indicate charge depletion [$\nabla^2 \rho(r) > 0$] and solid pink lines indicate charge concentration [$\nabla^2 \rho(r) < 0$].

SUPPORTING INFORMATION

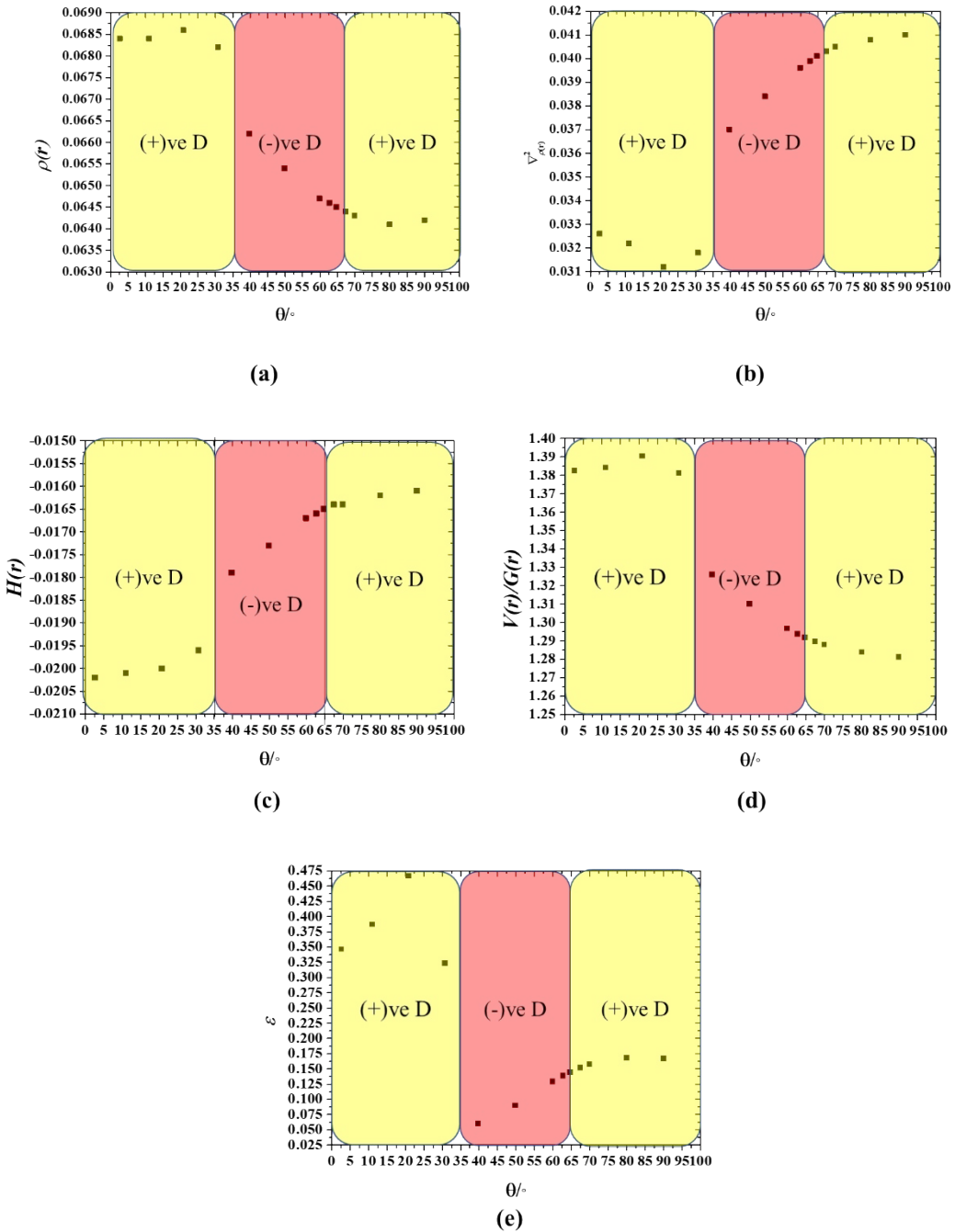


Fig. S10. Correlations between the QTAIM parameters and dihedral angle (a) $\rho(r)$ vs dihedral angle (b) $\nabla^2 \rho(r)$ vs dihedral angle (c) $H(r)$ vs dihedral angle (d) $|V(r)|/G(r)$ vs dihedral angle(e) ω vs dihedral angle. Also showing the mapping of the D values along different regions of AIM correlation.

SUPPORTING INFORMATION

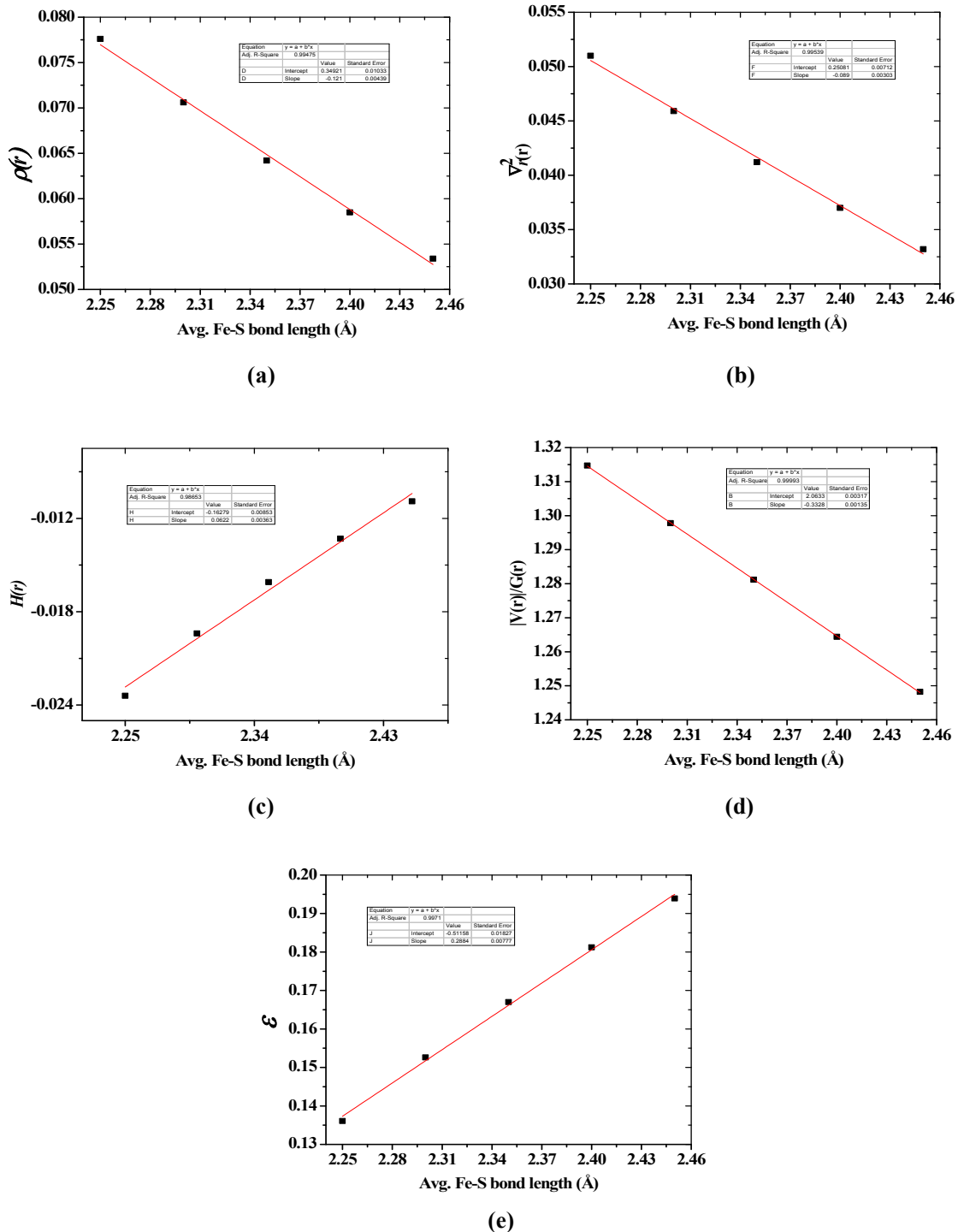


Fig. S11. Correlations between the QTAIM parameters and Fe-S bond length (a) $\rho(r)$ vs Fe-S bond length (b) $\nabla_{\rho(r)}^2$ vs Fe-S bond length (c) $H(r)$ vs Fe-S bond length (d) $|V(r)|/G(r)$ vs Fe-S bond length (e) ξ vs dihedral angle.

SUPPORTING INFORMATION

Table S14. Topological parameters at BCPs in the Fe–S bonds of the Complex **1**. All parameters are in a.u. $\rho(r)$ in units of $e\text{\AA}^{-3}$, G(r), V(r), H(r) in units of a.u.

Dihedral (θ_d)	Fe–S ₁ bonds							Fe–S ₂ bonds						
	$\rho(r)$	$\nabla_{\rho(r)}^2$	H(r)	G(r)	ε	V(r)	V(r) /G(r)	$\rho(r)$	$\nabla_{\rho(r)}^2$	H(r)	G(r)	ε	V(r)	V(r) /G(r)
B3LYP/TZV	0.0642	0.0412	-0.0161	0.0573	0.1670	0.0734	1.2812	0.0643	0.0406	-0.0163	0.0569	0.1507	0.0733	1.2870
B3LYP/def2-TZVP	0.0684	0.0429	-0.0184	0.0614	0.2058	0.0798	1.2996	0.0684	0.0429	0.0184	0.0614	0.2058	0.0798	1.2996
	Fe–S ₃ bonds							Fe–S ₄ bonds						
	$\rho(r)$	$\nabla_{\rho(r)}^2$	H(r)	G(r)	ε	V(r)	V(r) /G(r)	$\rho(r)$	$\nabla_{\rho(r)}^2$	H(r)	G(r)	ε	V(r)	V(r) /G(r)
B3LYP/TZV	0.0642	0.0409	-0.0162	0.0571	0.1664	0.0733	1.2840	0.0641	0.0411	-0.0161	0.0572	0.1759	0.0733	1.2816
B3LYP/def2-TZVP	0.0680	0.0429	-0.0183	0.0612	0.2097	0.0794	1.2973	0.0681	0.0430	-0.0183	0.0613	0.2186	0.0796	1.2985

SUPPORTING INFORMATION

References

1. M. Römelt, S. Ye and F. Neese, *Inorg. Chem.*, 2008, 48, 784-785.
2. (a)A. Becke, *J. Chem. Phys.*, 1993, 98, 5648;(b)C. Lee, W. Yang and R. G. Parr, *Physical review B*, 1988, 37, 785;(c)P. Stephens, F. Devlin, C. Chabalowski and M. J. Frisch, *The Journal of Physical Chemistry*, 1994, 98, 11623-11627;(d)M. J. Frisch, G. W. Trucks, H. B. Schlegel, G. E. Scuseria, M. A. Robb, J. R. Cheeseman, G. Scalmani, V. Barone, B. Mennucci, G. A. Petersson, H. Nakatsuji, M. Caricato, X. Li, H. P. Hratchian, A. F. Izmaylov, J. Bloino, G. Zheng, J. L. Sonnenberg, M. Hada, M. Ehara, K. Toyota, R. Fukuda, J. Hasegawa, M. Ishida, T. Nakajima, Y. Honda, O. Kitao, H. Nakai, T. Vreven, J. A. Montgomery, J. E. Peralta, F. Ogliaro, M. Bearpark, J. J. Heyd, E. Brothers, K. N. Kudin, V. N. Staroverov, R. Kobayashi, J. Normand, K. Raghavachari, A. Rendell, J. C. Burant, S. S. Iyengar, J. Tomasi, M. Cossi, N. Rega, J. M. Millam, M. Klene, J. E. Knox, J. B. Cross, V. Bakken, C. Adamo, J. Jaramillo, R. Gomperts, R. E. Stratmann, O. Yazyev, A. J. Austin, R. Cammi, C. Pomelli, J. W. Ochterski, R. L. Martin, K. Morokuma, V. G. Zakrzewski, G. A. Voth, P. Salvador, J. J. Dannenberg, S. Dapprich, A. D. Daniels, Ö. Farkas, J. B. Foresman, J. V. Ortiz, J. Cioslowski and D. J. Fox, Gaussian 09, revision D. 01, 2009.
3. R. Bader, Oxford, 1990.
4. R. F. Bader, *J. Phys. Chem. A*, 2009, 113, 10391-10396.
5. F. Biegler-König and J. Schönbohm, *J. Comput. Chem.*, 2002, 23, 1489-1494.
6. M. Pinsky and D. Avnir, *Inorg. Chem.*, 1998, 37, 5575-5582.